UKACC International Conference on Control 2012
Cardiff, UK, 3-5 September 2012

Model-base Predictive Control for Vibration Suppression of a Flexible Manipulator

Mehdi Abdolvand
Sama technical and Vocational Training College
Islamic Azad University, Islamshahr Branch
Islamshahr, Iran
Mehdi.abdolvand@gmail.com

Mohamad Hosain Fatehi
Department of Electrical Engineering
Islamic Azad University, Science and Research Branch
Tehran, Iran
Mh_fatehi@srbiau.ac.ir

***Abstract*—This paper focuses on the development of a multivariable predictive controller for vibration suppression of a flexible manipulator using piezoelectric actuator. To the best of the authors knowledge, the predictive controller for active vibration suppression has been rarely studied, so making it a prime area research to explore. A two-step procedure performed to develop the detailed model of the whole structure. First a dynamic model of the structure without piezoelectric film actuator is developed using the combined Lagrange-Assume modes method. Second the influence of the actuator is incorporated by calculating generalized applied force on the substructure.**

Keywords-Active Vibration Control; Flexible Structures; Model Predictive Control

I. INTRODUCTION

Design of flexible smart structures for vibration suppression and noise control represents a major challenge in the past two decades. Such structures are used in a variety of applications including robots, industrial machine design and tooling, aircraft systems, civil engineering structures and the space stations.

The flexible structures are generally lighter in weight, designed to use less material in order to be more transportable. They need less power for motion and therefore can be driven by smaller actuators resulting in less cost. Flexible structures are characterized by a significant number of closely spaced, lightly damped low frequency modes.

We focus on the algorithms which were recently developed and applied on motion control and active vibration damping of flexible structures. Lee and Moon [1] used two separate feedback loops for position and damping. They concluded that the controller is simple but robust, since it cancels out nonlinear and uncertain dynamics by acceleration feedback, and adds more damping by base motion feedback. Knotnic [2] used the linear quadratic regulator (LQR) and the acceleration feedback control method for vibration suppression. Chevallereau and Aoustin [3] applied nonlinear control laws for vibration control. Banks [4] used a linear quadratic Gaussian (LQG) compensator control with proper orthogonal decomposition to control a cantilever beam with a piezoelectric patch. Chen [5] applied the LQR algorithm and studied the optimum layout of the piezoelectric materials based on control performance specifications and a cost function. Robust control approaches such as H_∞ control design, robust pole assignment and D-stability constraints have often been applied to the problem of controlling large flexible space structures [6].

The strategies mentioned above all provide reasonable suppression of structural vibration. However, the feedback loop controller is difficult to apply to MIMO systems. Also, LQR and LQG controllers need a very accurate plant model for good control while the H_∞ controller can't easily handle multivariable constraints in the manipulated variables.

II. MODELING

A. Modeling of bending vibration

In this section the vibration of a flexible beam in the direction perpendicular to its length is considered. Such vibration is often called transverse vibration or flexural vibrations. Fig.1 illustrates a cantilevered beam with the transverse vibration [7].

From mechanics of materials, the beam sustains a bending moment M(x,t), which is related to the beam deflection by:

$$M(x,t) = EI_{cs} w_{xx}(x,t) \tag{1}$$

A model of bending vibration may be derived from examining the force diagram of an infinitesimal element of the beam as indicated in Fig. 1.

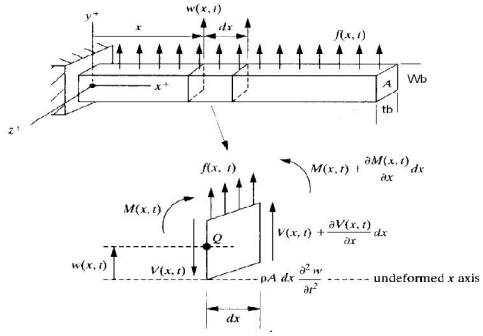

Figure 1. Simple beam in transverse vibration and a free body diagram of a small element as it is deformed by a distributed force

Assuming the deformation to be small enough such that the shear deformation is much smaller than w(x,t) so that the sides of the element dx do not bend, a summation of forces in the y direction yields:

$$\left(V(x,t)+\frac{\partial V(x,t)}{\partial x}dx\right)-V(x,t)+f(x,t)dx = \rho A\frac{\partial^2 w(x,t)}{\partial t^2}dx \tag{2}$$

Here V(x,t) is the shear force at the left end of the element dx, V(x,t)+V(x,t)dx is the shear force at the right end of the element dx, f(x,t) is the total external force applied to the element per unit length, and the term on the right side of the equality is the inertial force of the element.

Next the moments acting on the element dx about the z axis through point Q are summed. This yield:

$$\left(M(x,t)+\frac{\partial M(x,t)}{\partial x}dx\right)-M(x,t)+\left(V(x,t)+\frac{\partial V(x,t)}{\partial x}dx\right)dx+\left(f(x,t)dx\right)dx=0 \tag{3}$$

It is assumed that the rotary inertia of the element dx is negligible. Simplifying this expression yields ($(dx)^2$ is assumed to be almost zero):

$$V(x,t)=-\frac{\partial M(x,t)}{\partial x} \tag{4}$$

Substitution of this expression for the shear force into (2) yields:

$$-\frac{\partial^2}{\partial x^2}\left(M(x,t)\right)dx+f(x,t)dx=\rho A dx\frac{\partial^2 w(x,t)}{\partial t^2} \tag{5}$$

Further substitution of (1) into (5) and dividing by dx yields:

$$\rho A dx\frac{\partial^2 w(x,t)}{\partial t^2}+\frac{\partial^2}{\partial x^2}\left[EI_{cs}\frac{\partial^2 w(x,t)}{\partial x^2}\right]=f(x,t) \tag{6}$$

If no external force is applied so that f(x,t)=0 and (6) simplifies so that free vibration is governed by:

$$\frac{\partial^2 w(x,t)}{\partial t^2}+c^2\frac{\partial^4 w(x,t)}{\partial x^4}=0 \quad c=\sqrt{\frac{EI_{cs}}{\rho A}} \tag{7}$$

Equation (7) is based on the classical undamped Euler-Bernoulli beam theory.

To solve (7), w(x,t) can take the following expanded separated form with the chosen deflection mode shapes $\varphi_i(x)$ and the modal amplitudes $q_i(t)$:

$$w(x,t)=\sum_{i=1}^{\infty}q_i(t).\varphi_i(x) \tag{8}$$

By substituting (8) into the equation of motion (7) and after rearrangement yields:

$$c^2\frac{\varphi_i''''(x)}{\varphi_i(x)}=-\frac{\ddot{q}_i(t)}{q_i(t)}=\omega_i^2, \qquad c=\sqrt{\frac{EI_{cs}}{\rho A}} \tag{9}$$

where the partial derivatives have been replaced with total derivatives. (Note: $\varphi''''=d^4\varphi/dx^4, \ddot{q}=d^2q/dt^2$). ω_i is the natural frequency of vibration of mode i.

The spatial equation comes from rearranging (9), which yields:

$$\varphi_i''''(x)-\frac{\omega_i^2}{c^2}\varphi_i(x)=0, \qquad c=\sqrt{\frac{EI_{cs}}{\rho A}} \tag{10}$$

By defining:

$$\lambda_i^4=\frac{\omega_i^2}{c^2}=\frac{\rho A\omega_i^2}{EI_{cs}} \tag{11}$$

And considering the boundary conditions for this problem correspond to those of a clamped-free beam [8]:

$$\varphi_i(0)=0, \quad \frac{d\varphi_i}{dx}(0) \quad \frac{d^2\varphi_i}{dx^2}(L)=0, \quad \frac{d^3\varphi_i}{dx^3}(L)=0 \tag{12}$$

General solution of (10) can be obtained as:

$$\varphi_i(x)=\cosh(\lambda_i x)-\cos(\lambda_i x)-\sigma_i(\sinh(\lambda_i x)-\sin(\lambda_i x))$$
$$\sigma_i=\frac{\sinh(\lambda_i L)-\sin(\lambda_i L)}{\cosh(\lambda_i L)+\cos(\lambda_i L)} \tag{13}$$

The quantities $\lambda_i L$ are the real roots of the equation:

$$1+\cos(\lambda_i L)\cosh(\lambda_i L)=0 \tag{14}$$

These quantities determine the natural frequencies of the beam as follows:

$$\omega_i = \sqrt{\frac{EI_{cs}}{\rho A}} . \lambda_i^2 \tag{15}$$

Table (I) shows the calculated λ_i and ω_i for the first four modes of vibration. The temporal equation comes from rearranging (9), which yields:

$$\ddot{q}_i(t) + \omega_i^2 q_i(t) = 0 \tag{16}$$

A simple procedure for including damping is to add it to the temporal equation after separation of variables. So the modal damping can be added to (16) as follows:

$$\ddot{q}_i(t) + 2\xi_i\omega_i\dot{q}_i(t) + \omega_i^2 q_i(t) = 0 \tag{17}$$

Where ξ_i is the ith modal damping ratio. The damping ratios ξ_i are chosen based on experience or on experimental measurements. Empirical results in [8] show that the damping factor of the first mode is 0.01. The higher order modes were assumed to have the same damping factor. The solution, for an under damped mode becomes:

$$\begin{aligned} q_i(t) &= A_i e^{-\xi_i\omega_i t}\sin(\omega_{di}t + \Phi_i) \\ A_i &= \left[\frac{(\dot{q}_i(0) + \xi_i\omega_i q_i(0))^2 + (q_i(0)\omega_{di})^2}{\omega_{di}^2}\right]^{1/2} \\ \Phi_i &= \tan^{-1}\frac{q_i(0)\omega_{di}}{\dot{q}_i(0) + \xi_i\omega_i q_i(0)} \end{aligned} \tag{18}$$

Where A_i and Φ_i are constants to be determined by the initial condition. The robot link transverse displacement, approximately obtained, as a solution of the damped Euler-Bernoulli beam theory is finally expressed by [7]:

$$\begin{aligned} w(x,t) = \sum_{i=1}^{\infty} A_i e^{-\zeta_i\omega_i t}\sin(\omega_{di}t - \Phi_i)\times \\ \{\cosh(\lambda_i x) - \cos(\lambda_i x) - \sigma_i(\sinh(\lambda_i x) - \sin(\lambda_i x))\} \end{aligned} \tag{19}$$

B. Robot Dynamic Model

In order to obtain a set of ODE of motion to describe the dynamics of the flexible link manipulator, N differential equations must be satisfied [8]:

TABLE I. CALCULATED λ_i AND ω_i FOR FIRST FOUR MODES

Modes	λ_i	ω_i (rad/s)
First mode	1.8751	9.7474
Second mode	4.6940	61.0838
Third mode	7.8547	171.0406
Fourth mode	10.9955	335.1738

$$\frac{d}{dt}\left(\frac{\partial L}{\partial \dot{q}_i}\right) - \frac{\partial L}{\partial q_i} = Q_i \ , \ i = 1,\ldots,N+1 \tag{20}$$

Where L is the so called Lagrangian which is given by:

$$L = T - U \tag{21}$$

T represents the kinetic energy of the system and U its potential energy that can be found in [8]. The schematic of the system is shown in Fig. 2.

The joint angle θ and modal coordinates q_i can form a new vector $\tilde{q}$ of the system's generalized coordinates as:

$$\tilde{q}_{(N+1)\times 1} = [\theta\ q_1\ q_2 \cdots q_N]^T \tag{22}$$

Substituting the expressions for kinetic and potential energy into (20) and performing the required operations, one obtains the following matrix equation, which is a set of N+1 ode that model the dynamic behavior of the system:

$$M\ddot{\tilde{q}}(t) + H\dot{\tilde{q}}(t) + K\tilde{q}(t) = fv_m \tag{23}$$

v_m is the voltage applied to the motor. The mathematical derivation of the mass (M), damping (H) and stiffness (K) matrices also the expressions for energies of one link manipulator can be found in Appendix (B).The parameter f in (23) is defined as:

$$f_{(N+1)\times 1} = [k_u\ 0\ 0 \cdots 0]^T \tag{24}$$

where k_u is the torque constant and v_m is the voltage applied to the motor. The model in (23) does not include the effects of the piezoelectric films, which will be derived in the following section.

C. Analysis of Beam-Piezoelectric Interaction

Piezoelectric film could be used as an actuator or a sensor by applying a voltage or measuring the open circuit voltage, respectively. If the piezoelectric film is used as a sensor, the open circuit voltage of the sensor is given by [9] as:

$$V_{oc}(t) = \sum_{i=1}^{n} Q_i^{V_{oc}} q_i(t) \tag{25}$$

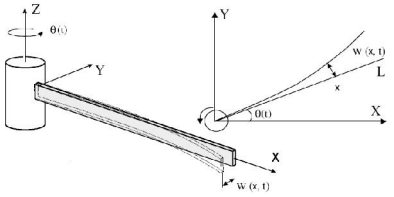

Figure 2. Schematic of the system

Where the ith modal coefficient is:

$$Q_i^{V_{oc}} = \frac{d_{31} E_c W_c t_b}{2C_c} \times \int_{a-m}^{a+m} \Xi_c(x) \frac{d^2 \varphi_i(x)}{dx^2} dx \qquad (26)$$

The physical characteristics of the beam and piezoelectric films and motor for simulations are given in Appendix A. The variable d_{31} is the transverse piezoelectric charge to stress ratio, E_c is the Young's modulus of the film, C_c is the capacitance of the piezoelectric film, $\Xi_c(x)$ is the shape function of the film, W_c is the maximum width of the piezoelectric film, t_b is the thickness of the beam. If the piezoelectric film is used as an actuator, its effect on the dynamic model is through the passive stiffness (negligible in this work) and the force produced by the actuator. The generalized force associated with ith mode is [9]:

$$F_i = f_i v_p \qquad (27)$$

v_p is the voltage applied to the actuator. The coefficient of the generalized force is defined as:

$$f_i = -\mathrm{sgn}(z_c) \frac{d_{31} E_c W_c t_b}{2} \left(\int_{r_s^n}^{r_e^n} \Xi_c(x) \frac{d^2 \varphi_i(x)}{dx^2} dx \right) \qquad (28)$$

Introducing the effect of piezoelectric films, the new system dynamic model can be described as:

$$M\ddot{\tilde{q}}(t) + H\dot{\tilde{q}}(t) + K\tilde{q}(t) = f_S v_m \qquad (29)$$

Where the new modal force coefficient matrix f_S, since one film were used as actuator in this work, becomes:

$$f_S = \begin{bmatrix} k_u & 0 & 0 & \dots & 0 \\ 0 & f_1 & f_2 & \dots & f_N \end{bmatrix}^T \qquad (30)$$

For modeling and control purposes it is convenient to write the model of the system in state-space form as follows:

$$\begin{aligned} \dot{x} &= Ax + Bu \\ y &= Cx \end{aligned} \qquad (31)$$

Where the matrices A and B are defined in terms of the stiffness, mass and damping matrices K, M and H, respectively, and the force vector f_S:

$$\begin{aligned} A &= \begin{bmatrix} [0]_{(N+1)\times(N+1)} & I_{(N+1)\times(N+1)} \\ -\left[M^{-1}K\right]_{(N+1)\times(N+1)} & -\left[M^{-1}H\right]_{(N+1)\times(N+1)} \end{bmatrix} \\ B &= \begin{Bmatrix} 0_{N\times 1} \\ \left\{M^{-1} f_S\right\}_{N\times 1} \end{Bmatrix}_{2N\times 1} \end{aligned} \qquad (32)$$

Where the state vector x includes the system's coordinates $\tilde{q}$ and $\dot{\tilde{q}}$ as:

$$x = \begin{bmatrix} \tilde{q} & \dot{\tilde{q}} \end{bmatrix}^T_{2(N+1)\times 1} \qquad (33)$$

The observation matrix C, which relates the state space to the output space, has to be obtained based on the available sensor. It includes the potentiometer encoder gain and the coefficients of the open circuit voltage for sensor that is expressed as:

$$C = \left[\begin{bmatrix} k_\theta & 0 & 0 & \dots & 0 \\ 0 & Q_1^{V_{oc1}} & Q_2^{V_{oc1}} & \dots & Q_N^{V_{oc1}} \end{bmatrix} [0] \right]_{2\times 2(N+1)} \qquad (34)$$

Where its second row is obtained by evaluating (26) with the parameters of the sensor patch [8].

III. CONTROLLER FORMULATION

Model-based predictive control (MPC) is based on the principle of minimizing an objective function J that contains a vector of future errors e over a prediction horizon p, resulting in changes on m control actions every sampling instant. The error vector e is evaluated as the difference between a prediction of each output variable of the process and a set point trajectory r. If the controller focuses exclusively on set point tracking, it might choose to make large manipulated-variable adjustments. These could be impossible to achieve. They could also accelerate equipment wear or lead to control system instability [10]. Thus, the Model Predictive Controller also monitors a weighted sum of controller adjustments, calculated according to the following equation:

$$\begin{aligned} J = &\begin{bmatrix} \Delta \underline{u}(0) \\ \dots \\ \Delta \underline{u}(p-1) \end{bmatrix}^T W_{\Delta u}^2 \begin{bmatrix} \Delta \underline{u}(0) \\ \dots \\ \Delta \underline{u}(p-1) \end{bmatrix} + \\ &\left(\begin{bmatrix} \underline{\hat{y}}(1) \\ \dots \\ \underline{\hat{y}}(p) \end{bmatrix} - \begin{bmatrix} \underline{r}(1) \\ \dots \\ \underline{r}(p) \end{bmatrix} \right)^T W_y^2 \left(\begin{bmatrix} \underline{\hat{y}}(1) \\ \dots \\ \underline{\hat{y}}(p) \end{bmatrix} - \begin{bmatrix} \underline{r}(1) \\ \dots \\ \underline{r}(p) \end{bmatrix} \right) \end{aligned} \qquad (35)$$

In this work, there are two inputs to the system, one to the motor v_m and one to the actuator v_p, and two outputs from the system, one is the motor or joint angular position which is measured by a high precision potentiometer that provides an analog voltage signal v_θ, the second is the beam vibration which is measured by a piezoelectric sensor that provides an analog voltage output v_{oc}. So in (35), $\underline{u} = [v_m, v_p]^T$, $\underline{y} = [v_\theta, v_{oc}]^T$, $W_{\Delta u}$ and W_y are weighting matrices as follows:

$$\begin{aligned} W_{\Delta u} &= \mathrm{diag}(w_{0,1}^{\Delta u}, w_{0,2}^{\Delta u}, \dots, w_{p-1,1}^{\Delta u}, w_{p-1,2}^{\Delta u}) \\ W_y &= \mathrm{diag}(w_{1,1}^{y}, w_{1,2}^{y}, \dots, w_{p,1}^{y}, w_{p,2}^{y}) \end{aligned} \qquad (36)$$

In this study, W_y has unit diagonal terms so that all future errors are equally weighted while the diagonal terms in $W_{\Delta u}$ are set to the move suppression. The general MPC architecture can be illustrated in Fig. 3. The future inputs $\{\Delta \underline{u}(k \mid k), \ldots, \Delta \underline{u}(m-1+k \mid k)\}$ (optimal sequence) are calculated by minimizing the cost function subject to the following constraints on inputs to the motor and actuator: $-50 \le v_m \le 50, -200 \le v_p \le 200$.

IV. Simulation Results

A. Open loop

The open loop response simulation due to a step input on the motor is shown in Fig. 4. The open loop response simulation due to a step input to the piezoelectric actuator is shown in Fig 5. It is clearly seen from the open loop test that the piezoelectric actuator has very little effect on the motor's joint angle and the sensor signal is oscillating with the beam's natural frequency.

B. Close loop

In the previous section we developed a model for the system to be controlled. In this section for simulation purposes we utilize a model as process for generating the data (see Fig. 3), considering four modes of vibration. Moreover the controller needs an approximate linear model to predict the future behaviors of the plant. We utilize a model as model predictor in Fig. 3 by considering only the first mode of vibration.

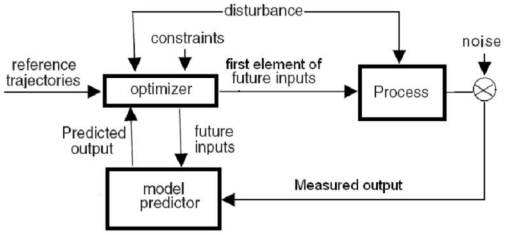

Figure 3. General MPC architecture

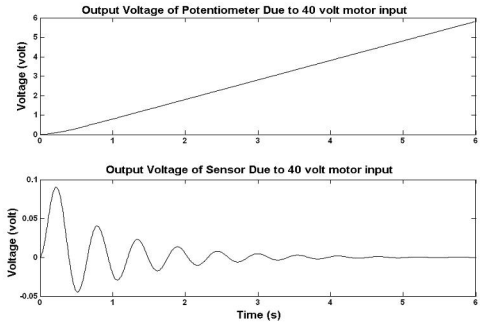

Figure 4. open loop test due to 40V motor input

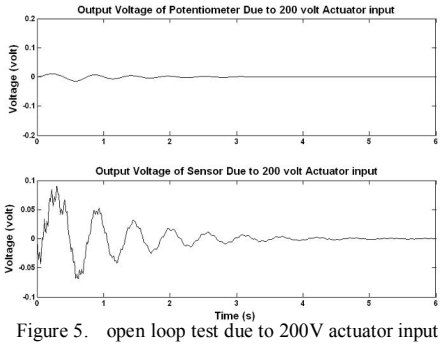

Figure 5. open loop test due to 200V actuator input

The value of prediction horizon p and control horizon m is based on the number of discrete sampling intervals required to reach within 95% of the plant output steady state. For many models, there is not much change beyond m=3~5, but p must be chosen as large as possible so that the value of p-m be greater than the settling time [11]. The motor is rotated and controlled to an angular set point using a multivariable predictive controller. During rotation, the beam's vibration is suppressed until angular rotation of the motor has been completed. Fig. 6 and Fig. 7 illustrate simulation results comparison between predictive control and conventional PI control when positioning the manipulator to 57 degree (assumed prediction horizon for both output is p=70 and the control move horizon for both inputs is m=5). It can be seen the vibration is suppressed by motor and piezoelectric actuator effectively. Predictive controller signal to motor and actuator are shown in Fig. 8.

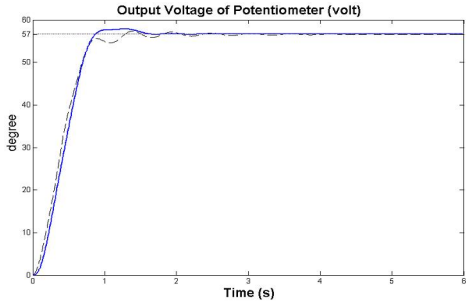

Figure 6. Joint angle comparison between MPC control (line) and PI control (dashed line)

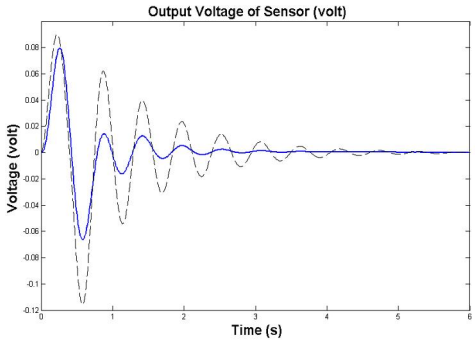

Figure 7. Displacement comparison between MPC control (line) and PI control (dashed line)

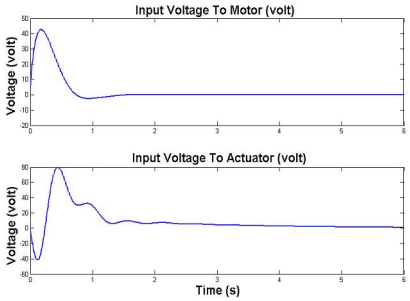

Figure 8. MPC controller signal to motor (upper) and to actuator (lower)Prepare Your Paper Before Styling

V. CONCLUSIONS

As stated in the introduction, the aim of this paper is to present a vibration control design methodology based on predictive control strategy. This methodology is illustrated by the design of a controller for a flexible cantilever beam. The advantage of this methodology over existing methodologies is that adjustments can be made on the prediction of beam vibration that takes into account the effects due to nonlinearities in the system. This study successfully demonstrates that predictive control can be applied to suppress vibration on a flexible beam, making it an excellent candidate for future research on topics such as intelligent control using an array of sensors and actuators, as well as controller tuning specifically for other applications such as a multi-jointed flexible structures.

APPENDIX A

This appendix contains the parameter values for the beam, motor and piezoelectric films.

TABLE II. BEAM PROPERTIES

Material	Aluminum
Density ρ (Kg/m^3)	2700
Young's modulus E (N/m^2)	6.9×10^{10}
Length×Width×Thickness (m)	1×0.035×0.0019

TABLE III. MOTOR PROPERTIES

Motor fixture inertia J_h (Kg.m^2)	0.14
Friction coeff. B_m (Nm/rad)	0.95
Motor torque constant k_u (Nm/V)	0.06
Encoder gain k_θ (V/rad)	0.3979

TABLE IV. PIEZOELECTRIC FILM PROPERTIES

parameters	Sensor	Actuator
Charge constant d_{31} (C/N)	23×10^{-12}	175×10^{-12}
Young's modulus E_c (N/m^2)	2×10^{9}	6.5×10^{10}
Length×Width×Thickness (mm)	250×35×1	150×35×1
Capacitance C_c (F)	2.7×10^{-6}	2×10^{-8}
Shape function Ξ_c	1	1

APPENDIX B

$$M=\begin{bmatrix} J_h+\frac{\rho AL^3}{3} & \rho A\int_0^L \varphi_1(x)xdx & \rho A\int_0^L \varphi_2(x)xdx & \cdots & \rho A\int_0^L \varphi_N(x)xdx \\ \rho A\int_0^L \varphi_1(x)xdx & \rho A\int_0^L \varphi_1^2(x)dx & 0 & \cdots & 0 \\ \rho A\int_0^L \varphi_2(x)xdx & 0 & \rho A\int_0^L \varphi_2^2(x)dx & \cdots & \vdots \\ \vdots & \vdots & \vdots & \ddots & \vdots \\ \rho A\int_0^L \varphi_N(x)xdx & 0 & \cdots & \cdots & \rho A\int_0^L \varphi_N^2(x)dx \end{bmatrix}_{(N+1)\times(N+1)}$$

$$K=\begin{bmatrix} 0 & 0 & 0 & \cdots & 0 \\ 0 & EI_{cs}\int_0^L (\varphi_1''(x))^2dx & 0 & \cdots & 0 \\ 0 & 0 & EI_{cs}\int_0^L (\varphi_2''(x)^2)dx & \cdots & 0 \\ \vdots & \vdots & \vdots & \ddots & \vdots \\ 0 & 0 & 0 & \cdots & EI_{cs}\int_0^L (\varphi_N''(x))^2dx \end{bmatrix}_{(N+1)\times(N+1)}$$

$$H=\begin{bmatrix} B_m & 0 & 0 & \cdots & 0 \\ 0 & 2\zeta_1 m_{22}\omega_1 & 0 & \cdots & 0 \\ 0 & 0 & 2\zeta_2 m_{33}\omega_3 & \cdots & 0 \\ \vdots & \vdots & \vdots & \ddots & \vdots \\ 0 & 0 & 0 & \cdots & 2\zeta_N m_{N+1,N+1}\omega_N \end{bmatrix}_{(N+1)\times(N+1)}$$

REFERENCES

[1] C. K. Lee, F.C. Moon, "Modal Sensors/Actuators," J. Appl. Mech., 1990, Vol. 57, No. 2, pp. 434-441.

[2] P.T. Knotnic, S. Yurkvocich, U. Ozguner, "Acceleration Feedback for control of a Flexible Manipulator Arm," J. Robotic Syst., 1988, Vol. 5, No. 3, pp. 181-196.

[3] Y. Aoustin, C. Chevallereau, A. Glumineau, C.H Moog, "Experimental Results for the End-Effector control of a Single Flexible Robotic Arm," IEEE Trans Contr.Syst. Technol, 1994, Vol. 2, No. 4, pp. 371-381.

[4] H.T. Banks, R.C.H Del Rosario, H.T. Tran, "Proper Orthogonal Decomposition-Based Control of Transverse Beam Vibrations: Experimental Implementation," IEEE Trans Contr. Syst. Technol, Sep. 2002, Vol. 10, No. 5, pp. 717-726.

[5] Wei Chen, Markus Buehler, Gordon Parker, and Bernhard Bettig, "Optimal Sensor Design and Control of Piezoelectric Laminate Beams," IEEE Trans Contr. Syst.Technol., Vol. 12, No. 1, pp. 148-155, Jan. 2004.

[6] J. Daafouz, G. Garcia, and J. Bernussou, "Rubust Control of a Flexible Robot Arm Using the Quadratic D-Stability Approach," IEEE Trans Contr. Syst. Technol ., Vol.6, pp. 524-533, Sep. 1998.

[7] Daniel J. Inman, Engineering Vibration.Prentice-Hall, second edition 2000.

[8] R . Bravo, Vibration Control of Flexible Structures Using Smart Material, PhD. Dissertation, McMaster University,Canada,2000.

[9] A.F. Vaz, "Composite Modeling of Flexible Structures with Bonded Piezoelectric Film Actuators and Sensors," IEEE Trans on Intrumentation and Measurement, April 1998,Vol. 47,No. 2, pp.513-520.

[10] J.M. Maciejowski, Predictive Control with constraints, Prentice-Hall, first edition 2000.

[11] Camacho, Eduardo. Bordons, Carlon. Model Predictive Control, Springer, first edition 1999.